ASPECTS OF DIGITAL ELEVATION MODEL DETERMINATION

John C. Trinder, Ping Wang, Yi Lu, ZhijunWang, Eric D. Cheng

School of Surveying and Spatial Information Systems
The University of New South Wales, Sydney, Australia
j.trinder@unsw.edu.au

Invited Paper – Commission IV

KEY WORDS: Digital Elevation Models, Kalman filtering, Wavelets, Image Matching, Image Processing, Interferometry.

ABSTRACT:

The paper describes aspects of research being undertaken on the determination and processing of digital elevation models. A 2-D Kalman filter has been developed based on dynamic and functional models for a grid DEM, to produce optimal estimates of terrain attributes of a DEM point using the relevant observations, and predictions derived from its orthogonal neighbouring points. A further method of filtering DEMs based on Wavelets has been developed to compare it with the efficiency of the Kalman filtering method. An intelligent DEM procedure under development comprises several components using image processing, image understanding and terrain modelling. These include the recognition of some buildings on the terrain and the correction of errors in the elevations caused by these buildings, recognition of areas of vegetation on the terrain surface, which will lead to poor quality image matching and hence erroneous elevations. In addition, the geomorphology of the terrain surface, based on the drainage patterns are being derived from the computed DEMs. Further, ERS1/2 Tandem SAR data has been tested as an appropriate data set for upgrading the national digital elevation database over Australia.

1. INTRODUCTION

Digital Elevation Models (DEM) are essential for many aspects of terrain and environmental modelling. They are available in a number of different forms, either as contours on hardcopy maps, digitized contours, and digitized regular or irregular grids. The types of DEMs required by users are often specifically related to their applications. For example, the spacing and accuracy of a user of DEMs who wishes to investigate the natural drainage system of a suburban area requires a different resolution and accuracy DEM than a person who is interested in studying the likelihood frosts in an area. Therefore, users of DEMs often find that the accuracy of available DEMs are inadequate for their purposes and hence they are required to acquire new DEMs at considerable cost, or adapt those available, even though they may be inadequate for their purposes. In addition, users often acquire data from various sources, such as digitized contours without adequate records of the lineage of the data, or indeed even an accuracy statement on the data. Using this data often results in what geographers call 'sinks or depressions' and 'mounds' in the DEM data. This data usually requires editing or smoothing to enable them to be useful.

Photogrammetrists derive DEMs from analogue or digital images and have a good knowledge of the accuracy of the data they derive. They usually do not considered such processes as terrain modelling and drainage pattern delineation within their area of interest, yet the design of theoretical sound methods of DEM processing should be an important task for the people who derive the data. People acquiring DEM data should also be aware of the needs of the users of their data, such as geographers, engineers and environmentalists. Since available DEMs are often inadequate for applications of users, there is a need to develop methods of data acquisition that are cheaper and faster, as well as methods of processing the data, and methods of quality assessment and assurance of DEMs. Digital photogrammetric methods of DEM acquisition have been developed over the last 10 years because of improvements of computer and display technologies. The methods are rapid in terms of the number of points that can be acquired per minute, but they suffer from significant errors caused by such aspects as poor correlation between the images, and buildings and trees on the terrain surface. The time taken to correct the errors in the data often means that the digital methods are only marginally more efficient than the manual methods, or indeed they may even be less efficient if the editing required is lengthy. Considering these issues related to DEMs, this paper describes research on processing and acquisition of DEMs, including procedures for noise reduction by Kalman filtering and Wavelets, the correction of digitally derived DEMs for errors caused by buildings and trees, the extraction of geomorphological parameters, such as drainage patterns as a process of ensuring the quality of determination of digitally derived DEMs, and the determination of elevations from ESA Tandem Mission SAR data by interferometry (InSAR).

2. DEM FILTERING

The 2-D Kalman filter is based on dynamic and functional models for a grid DEM to produce optimal estimates of terrain attributes of a DEM point using the relevant observations, and predictions derived from its orthogonal neighbouring points. It was developed to filter discrepancies in DEMs that may occur due to trees and similar objects on the terrain, thereby generating accurate terrain topographic attributes in gird DEMs (Wang 1998). The output of the process are the estimates of elevation, and the first order of partial derivatives of elevation (ie slopes in E and N directions).

2.1 2-D Kalman Filtering of DEMs

This technique uses the neighbouring DEM points, $p(i-1, j)$ and $p(i, j-1)$, to model any arbitrary point $p(i, j)$. For example, in X direction,

$$H(i,j) = H(i-1,j) + H_x(i-1,j)dx + v_{H_b}(i,j) \quad (1)$$

$$H_x(i,j) = H_x(i-1,j) + v_{H_{x_b}}(i,j) \quad (2)$$

$$H_y(i,j) = H_y(i-1,j) + v_{H_{y_b}}(i,j) \quad (3)$$

Where $H(i,j)$, $H_x(i,j)$, and $H_y(i,j)$ are the elevation, the first partial derivatives of elevation along the X and Y directions of point (i,j) respectively. $H(i-1,j)$, $H_x(i-1,j)$, and $H_y(i-1,j)$ are the elevation, the first partial derivatives of elevation along the X and Y direction of point $(i-1,j)$ respectively. dx is the sampling intervals of the DEM in X direction. v_{H_b}, $v_{H_{x_b}}$, and $v_{H_{y_b}}$ are assumed as white noise sequences, which are to be filtered. An additional three equations were formed in the Y direction.

The 2-D recursive process developed, based on these equations, has shown to be suitable for handling DEM random noise during the terrain modelling process. A DEM outlier detection and removal is an extra function that is added to the 2-D Kalman filter developed in this research. It uses the dispersions between the predicted estimates of elevation and the relevant elevation observations to detect outliers. In addition, a 2-D Kalman smoother is a linear combination of four 2-D Kalman filtering results, derived on the basis of different orientations, that further improves the accuracy of the 2-D Kalman filtering process. The methods have been applied experimentally on a simulated and a real world DEM and proved to be more efficient than existing methods.

2.2 DEM Filtering by Wavelet Transform

Wavelet transforms (WT) have furnished new approaches for describing and modelling the data. Using wavelets, a signal can be split into two or more bands. There are many 2D wavelet transform algorithms available. The most frequently used methods are two fast computation algorithms Mallat algorithm and á trous algorithm. Mallat's algorithm is based on the principle of reducing the redundancy of the information in the transformed data. The processing of decimating in the Mallat algorithm induces the phase distortion which results in edge shift, so it should not be employed to remove noise in DEMs. Á trous algorithm is shift-invariant, which can decompose the original signal into its approximation and its wavelet components at the same scale, and hence can deal with DEM noise removal. Its application to DEM error filtering and its influence on drainage network extraction will be considered in this paper.

2.2.1 Á Trous algorithm Wavelet transform based filtering strategy concerns both the wavelet transform algorithm used, and the processing carried out on the wavelet coefficients. Different strategies can be employed to remove noise from DEMs. Starck et al (2002) compared four wavelet transforms algorithms and eight different strategies for the processing carried out on the wavelet coefficients. Among those transforms, Á trous algorithm does not create artifacts when thresholding and results are significantly better. As opposed to the standard WT method, this transform is isotropic and performs better on isotropic structures.

Á trous algorithm was introduced to decompose the image into wavelet planes [Wang Zhijun, 2000]. Given an image *p*, we can construct the sequence of approximations: $F_l(p) = p_1$, $F_2(p) = p_2$ …, The wavelet planes are computed as the differences between two consecutive approximations:

$$w_l = p_{l-1} - p_l, (l = 1...n), p_0 = p \quad (4)$$

we can write the reconstruction formula as:

$$p = p_r + \sum_{l=1}^{r} w_l \quad (5)$$

r refers to the decomposition level.

The discrete filter h is derived from the scale function $\phi(x)$. In our calculations, we select the filter h as a Lagrange Á trous filter, which is in one-to-one correspondence with the convolutional squares of the Daubechies filters for orthogonal wavelets of compact support (Shensa 1992). It is derived by the convolution of an analysis lowpass filter and a reconstruction lowpass filter of Daubechies filter.

2.3. Drainage Network Extraction

Drainage patterns can be used as a means of checking the quality of the derived DEMs and correction of errors that have occurred in the extraction process. There are a number of algorithms available for extracting drainage network from grid based DEM. Basically, all the methods can be classified into two groups: terrain surface geometrical analysis and terrain surface water-flow analysis. In our project, we have used the terrain surface water-flow analysis algorithm based on ARC/INFO grid model. It determines the water flow direction and flow accumulation of each grid segment in the DEM. The flow direction is the steepest slope in each grid segment. Accumulated flow can be computed from the weighted sum of the flow into each down-slope grid segment. Grid segments with a high flow accumulation are areas of concentrated flow and may be used to identify stream network, while segments with a flow accumulation of zero are local topographic highs and may be used to identify ridges. Small depressions have to be smoothed out as they can be seen as errors in the elevations, and can cause serious problems in flow routing. They should be removed by noise reduction methods before the computation of flow direction. Depressions or sinks cannot be simply removed by noise removal, ARC/INFO provides the tools to remove depressions and produce a 'depressionless' DEM.

2.4. Experiments on Drainage Network Extraction

In our research, we have investigated a strategy to remove the DEM noise by wavelet transform, and extracted the drainage networks from the original DEM and the smoothed DEM. We extracted the DEM dataset automatically by L-H Systems digital photogrammetric workstation with a grid space of 5m, a total of 228 x 283 = 64524 points. Figure 1 is the 3D perspective view of the area.

After applying á trous algorithm on the original DEM, the smoothed DEM is shown in Figure 2. Profiles of the original and smoothed DEMs and the overlay of both are shown in Figure 3, from which it can be concluded that á trous algorithm gives a good smoothed result. The original and smoothed DEMs were then transferred into ARC/INFO GRID module, using functions *flowdirection* and *flowaccumulation*.

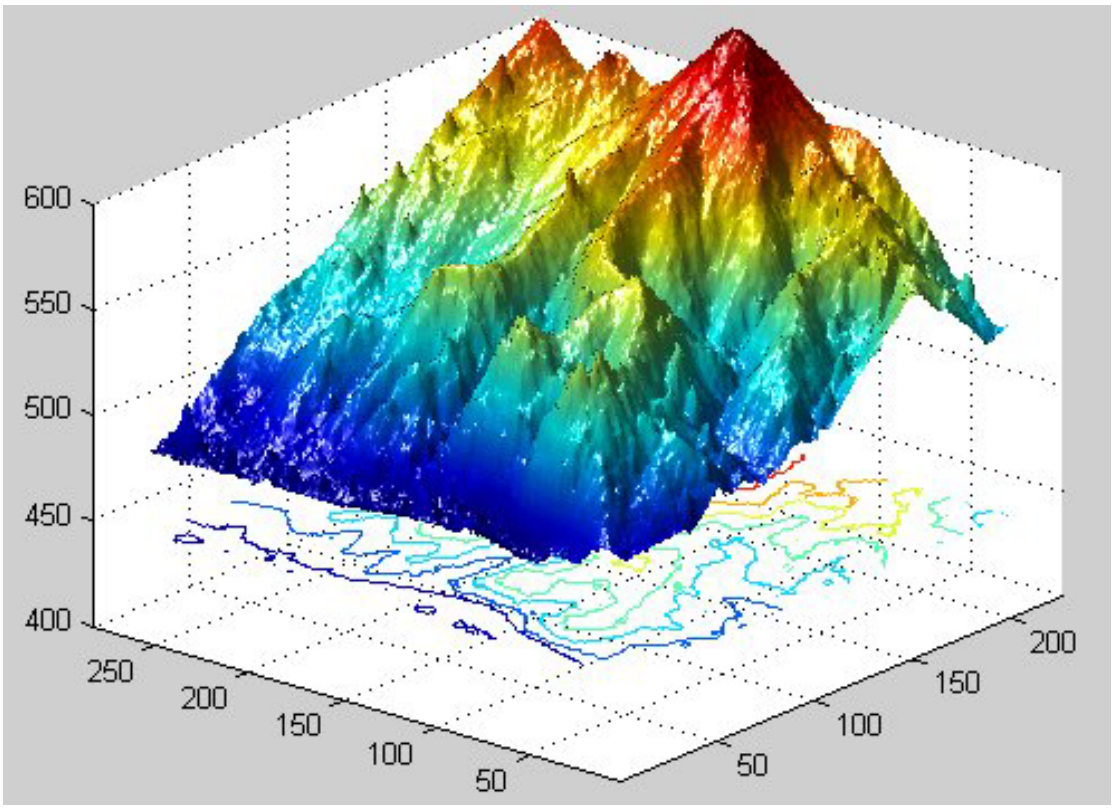

Figure 1. 3D perspective view of original DEM

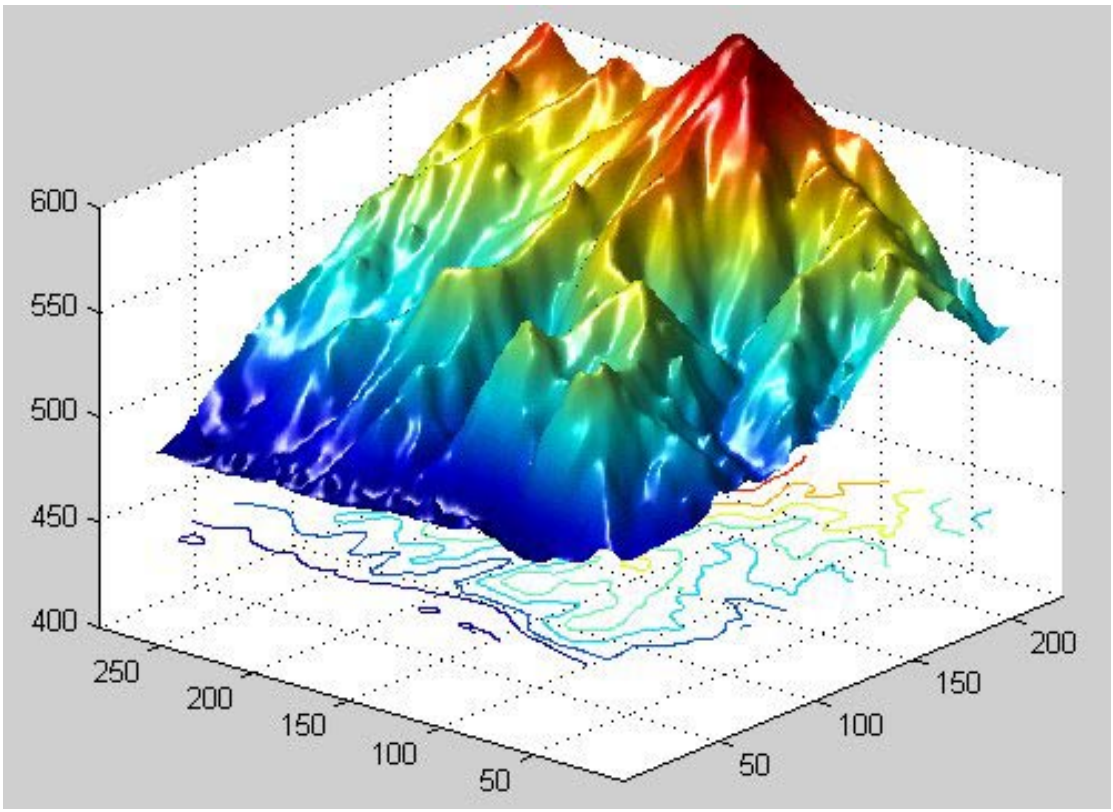

Figure 2. 3D perspective view of Wavelet transform smoothed DEM

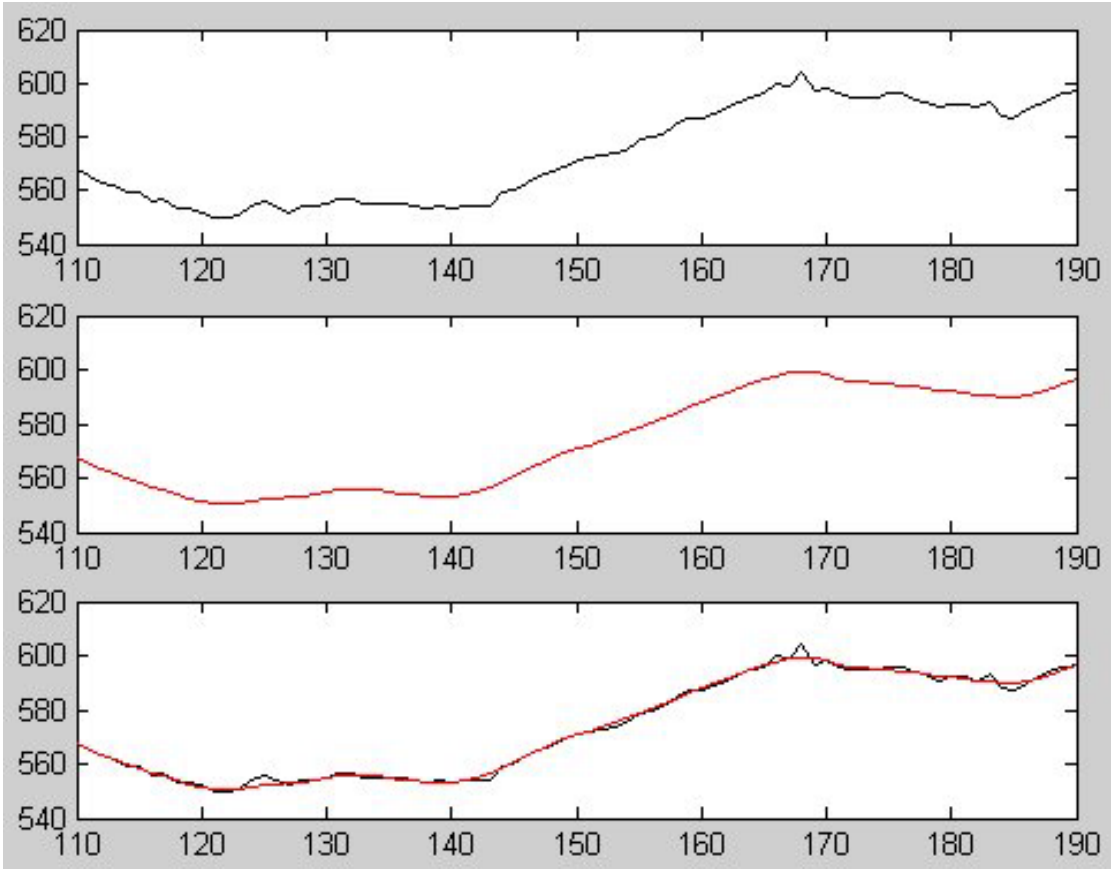

Figure 3: Profiles of the original DEM, Wavelet Transform smoothed DEM and its overlay

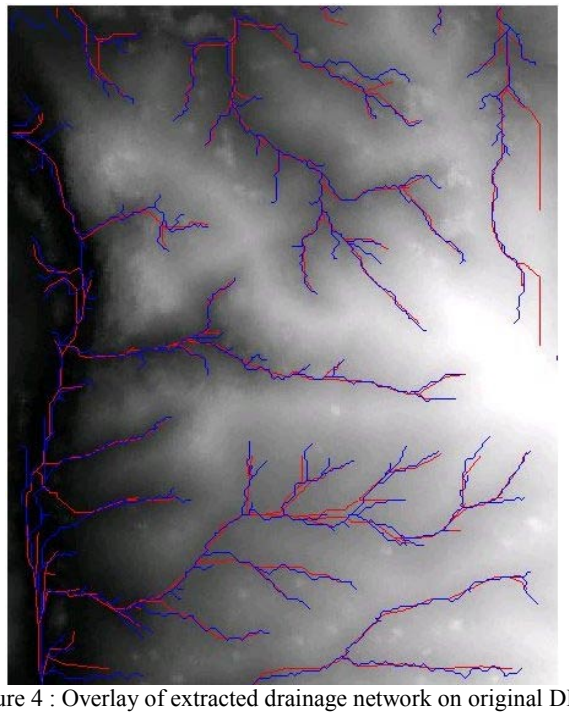
Figure 4 : Overlay of extracted drainage network on original DEM
Red: Drainage network from smoothed DEM
Blue: Drainage network from original DEM

The result of the drainage network extraction is dominated by the threshold, which we have found should be defined according to the terrain roughness. The extracted drainage networks are checked by visual inspection as displayed on the DEM in Figure 4, the red layer being extracted from the smooth DEM and the blue layer, from original DEM. The red layer is smoother than the blue layer, but both fit the DEM well, except in some areas around the boundaries, which are influenced by filtering processing. More detailed data quality check of the extracted drainage network is under investigation.

3. TOWARDS INTELLIGENT DEM DETERMINATION

In digital photogrammetric systems for DEMs computation, elevations are usually located at discrete posts, with little reference to the elevations in neighbouring posts and hence may be subject to errors caused by poor definition of terrain features in the image. An intelligent DEM procedure under development comprises several components using image processing, image understanding and terrain modelling. These processes are designed to recognize some buildings and correct errors in the elevations caused by these buildings, to recognize areas of vegetation on the terrain surface which will lead to poor quality image matching and hence erroneous elevations, and the extraction of terrain morphology, as described above.

3.1 General Description of Automatic Extraction of Building System

Figure 5 illustrates the architecture of an automatic building extraction system. The goal of this technique is to achieve accurate building boundaries for reconstruction of elevations from overlapping aerial or satellite images over a wide variety of terrain types and ground cover. The system consists of two main parts. Part 1 performs the matching of the stereo image pair, derives a disparity map, and produces a digital surface model (DSM). An analysis of multispectral (colour) images then supplies multi-band classification, and segmentation of classification, based on the Normalised Difference Vegetation Index (NDVI). These four information layers finally produce building areas. Part 2 applies a level set formulation of curve and surface motion to obtain an initial curve indicating the desired building boundary, driven by an image-dependent speed function.

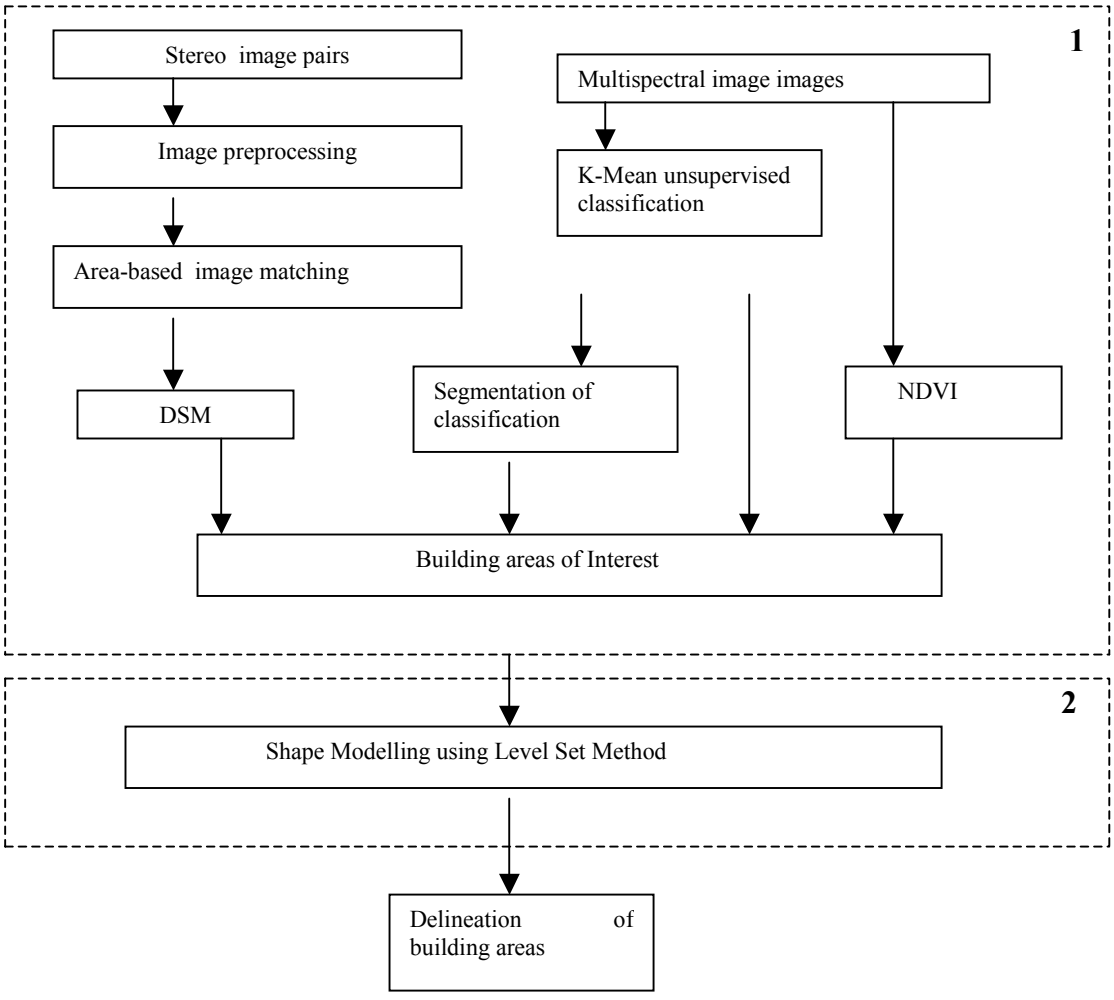

Figure 5 Architecture of the building extraction system

3.2 Processing of Stereo and Colour Images

3.3.1 DSM Derivation The first step in the recovery of 3D terrain information from overlapping aerial or satellite images is based on the matching of corresponding pixels in the stereo images. Since this paper concentrates on the process of recognizing buildings in images, the DSM was obtained from L-H Systems Socet Set. A dense sample of points in the DSM is required in order to avoid missing some of structures.

3.3.2 Multispectral Processing Ideally the classification of terrain cover should be undertaken with multispectral imagery. However, most multi-spectral images have insufficient resolution for the location of buildings and trees that occur in aerial photography. Therefore the study had to be restricted to scanned colour aerial photography. Multispectral image classification can be used to detect individual object primitives. It should also be helpful to reduce the complexity for the next processing step for object structure detection. To locate building areas, an iterative K-Means unsupervised classification was used. The NDVI (Vegetation Index) was then used to identify green vegetation.

Simplistically, areas which have heights above a certain limit are likely to be either trees or buildings. Areas with low NDVI, which are above the surface are likely to be buildings, whereas areas with high NDVI, and which are above the surface are likely to be trees. Areas with high NDVI and located at the bare earth surfaces are likely to be grassland or cultivated areas. Four information layers, the land cover classification, segmentation of classification, DSM and NDVI, are therefore combined to locate final building areas.

3.3.3 Location of Building Outlines The level set method for propagating interfaces was introduced by Osher and Sethian (1988). It is based on mathematical and numerical work of curve and surface motion by Sethian (1985) and offers a highly robust and accurate method for tracking interfaces moving under complex motions. Consider a closed curve moving in the plane. Let $\gamma(0)$ be a smooth, closed initial curve in Euclidean plane R^2, and let $\gamma(t)$ be the one-parameter family of curves generated by moving $\gamma(0)$ along its normal vector field with speed $F(K)$, K is a given scalar function of the curvature. Let $\boldsymbol{x}(s,t)$ be the position vector which parameterises $\gamma(t)$ by s, $0 \le s \le S$.

One numerical approach to this problem is to take the Lagrangian description of the problem. One can produce equations of motion for the position vector $\boldsymbol{x}(s,t)$, and then determine the parameterisation with a set of discrete marker particles lying on the moving front. These discrete markers are updated in time by approximating the spatial derivatives in the equations of motion, and advancing their positions. The detailed equations can be found in (Sethian 1999). However, there are several problems with this approach.

- Small errors in the computed particle positions are highly amplified by the curvature term, and calculations become unstable, unless an extremely small time step is employed.
- In the absence of a smoothing curvature term, singularities develop in the propagating front, and an entropy condition must be observed to extract the correct weak solution.
- The topological changes are difficult to manage as the evolving interface breaks and merges.
- Significant problems occur in the extension of this technique to three dimensions.

The level set method has been applied to solve the above problems. Level set method represents the front $\gamma(t)$ as the level set $\{\Phi = 0\}$ of a function Φ. Thus, given a moving closed hypersurface $\gamma(0)$, we produce a formulation for the motion of the hypersurface propagating along its normal direction with speed *F*. *F* can be a function of various arguments, including the curvature, normal direction, etc. Further developments of this method will not be given in this paper.

3.2 Test and Results

Figure 6 illustrates a pair of aerial images with 580 × 560 pixels in the row and column directions respectively. The focal length of the camera is 153mm, flying height is 3070m, and the ground resolution is 0.3m. Figure 7 illustrates the DSM image obtained from stereo images. Results of the unsupervised classification using K-Means method are given in Figure 8, where yellow is assigned to building areas, red and green show vegetation areas and blue indicates roads. Based on the classification of Figure 8, using a post classification procedure, a segmentation image can be created to show the building areas as illustrated in Figure 9. The Normalized Difference Vegetation Index values are shown in Figure 10.

Four information layers of Figures 7, 8, 9, and 10 are combined to locate the final building areas are shown in Figure 11. Using a region growing algorithm, the small areas which do not belong to buildings can be deleted from the Figure 11. Further processing is then undertaken using the routine based on the level set to define the outlines of the buildings. The building outlines are then combined with the building areas in Figure 11 to accurately define the buildings. Once the building areas are located, they can be deleted from the DSM to derive the correct DEM of the terrain surface.

4. DEMS BY INTERFEROMETRY FROM TANDEM MISSION DATA

In April 1995 the European Space Agency (ESA) launched its second earth observation satellite, ERS2, which like the first satellite, ERS1, included a C-band Synthetic Aperture Radar (SAR) remote sensing imaging system. The 35 day orbits of the two satellites were programmed for the Tandem Mission, so that there was a 1-day interval between the times ERS1 and ERS2 looked at the same area on the Earth. The ERS Tandem Mission commenced on the August, 1995 and operated until May1996. It provided vast amounts of data that can be used for a number of applications in the geosciences industry, based on the principle of interferometry, (InSAR). InSAR techniques provide a new method of deriving DEMs with little manual input over almost all of the global land surface (including Antarctica). The main objective of the Tandem Mission, was to acquire a unique and valuable set of SAR data that could be used for InSAR purposes. ERS1/2 Tandem SAR data is considered an appropriate data set for upgrading the elevation data over Australia, and hence tests were carried out on the quality of the elevations that can be derived from this dataset.

Figure 6 Stereo aerial images

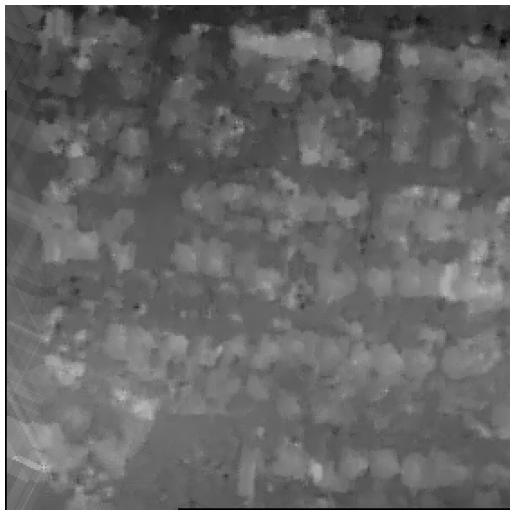

Figure 7 DSM from stereo image matching

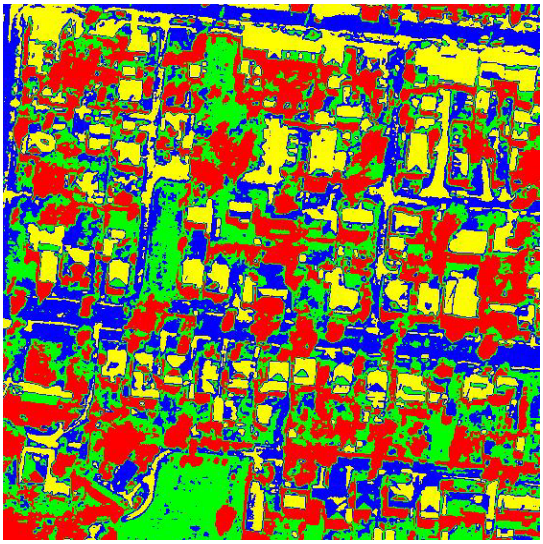

Figure 8 Unsupervised classification

Figure 9 Building areas from Figure 9

Figure 10 NDVI image

Figure 11 The building areas overlapped on ortho image

4.1 Description of Tests in InSAR Data

The aims of this project were to test the suitability of the method of InSAR, using the ERS1/2 Tandem Mission data for achieving greater efficiencies in upgrading the digital elevation model (DEM) data in Australia. In addition, the objectives were to develop practical methods of using InSAR techniques on the Tandem Mission data in a production environment. The study has involved the use of two software packages, Atlantis EarthView™ and Phoenix Systems Pulsar™, for processing the Tandem ERS1/2 data. A third package, Vexcel is also available in Geoscience Australia. Tests were carried out on 13 image pairs of Tandem Mission data, some of which overlap with each other. The procedure for computation of DEMs involved the determination of the coherence between the pairs of images, referred to as master and slave images, the computation of the interferograms from the phase information of the pixels, phase unwrapping to convert the interferogram values to elevations. In the case of the Atlantis EarthView™ software it was then necessary to locate Ground Control Points (GCPs) to reduce the elevations to the height datum. The maps available for the identification of the GCPs varied from 1:25,000 to 1:100,000, which meant that the elevations of the GCPs had accuracies varying from 3m to 8m. The selection of GCPs was a difficult task, since the identification of map features on the radar images, where their appearance depended on the reflectance characteristics of the terrain surface, presented problems. A maximum of 100-200 GCPs were usually identifiable on the maps and an image pair. PulSAR software did not require the use of GCPs, since it uses the satellite ephemeris to locate the DEM on the terrain surface. If required the precise ephemeris can also be obtained from ESA to improve the positioning of the DEM. PulSAR also uses a coarse DEM of the area to assist in the phase unwrapping and provide the initial values of the DEM.

The mean errors and estimated accuracy of DEMs in this study were determined by comparing the computed elevations of the GCPs and check points located manually on existing topographic maps, with their known values, and also by overlaying the derived DEM onto a known DEM. The known DEM available is the AUSLIG 9" DEM national database of Australia with an estimated accuracy of about 10m. In all cases in these tests, accuracies were quoted as the RMS of the differences between the elevations derived from topographic maps of the area, or the known DEM of the area, and the computed elevations by interferometry.

4.2 Achieved Accuracy of DEMs by InSAR

Conditions found necessary for determination of DEMs from InSAR are as follows:

- The perpendicular baseline between the orbits of the two data passes should be less than 300m, preferably 100-200m
- Ground control points should be available for Atlantis software with an accuracy compatible with the expected accuracy of the computed elevations
- Good coherence between the pairs of images is required, otherwise large elevation errors will occur
- The terrain conditions for the two acquisitions should not vary significantly, otherwise temporal decorrelation will render the images unsuitable for InSAR applications.

As a result of the tests using PulSAR software on full scenes (110kmx40km), accuracies of elevations of the order 10m were achievable with the InSAR technique from ERS1/2 Tandem Mission data, based on the mean of elevations obtained from at least two pairs of images of the same area. Individual pairs of images resulted in accuracies of the order of 15m, but on some occasions poorer accuracies occurred. The accuracies achieved are comparable with similar tests in Europe, based on the use of ERS1/2 Tandem data. In some cases large errors existed in the computed DEM, but these were always in areas where coherence between the two images was low and the elevations of many points in the same region could not be determined satisfactorily.

Altantis software resulted in significantly lower accuracy elevations, of the order of 30m for a full scene and 10-15m for areas of ¼ of a scene. However, the need to use GCPs reduced the accuracy of the elevations and slowed the process very significantly. For many parts of Australia, a sufficient number of accurate GCPs would not be available from existing maps to provide control for Atlantis software.

5. FINAL REMARKS

This paper has given a review of research being undertaken on DEMs at UNSW. Given the importance of elevation data as an layer in GIS, to many activities involving a study of terrain form, such as civil engineering, environmental monitoring and terrain modelling, efficient methods of data acquisition, as well as data quality assurance, require investigation and development. Some aspects of these issues have been presented in this paper, including, filtering DEMs, determination of terrain cover and terrain morphology to increase the intelligence of the DEM acquisition process, and the computation of elevations from a readily available data source, the ESA ERS1/2 Tandem Mission SAR data by interferometry.

6. REFERENCES

Osher S. & Sethian J.A. (1988) "Fronts propagating with curvature dependent speed: Algorithms based on Hamilton-Jacobi formulation", *J. of Computational Phhysics*, Vol. 79, pp.12-49.

Sethian J. A. (1985) "Curvature and the evolution of fronts", *Comm. In Math. Phys. 54,* pp.87-499.

Sethian J. A. (1999) " Level set methods and fast marching methods", Cambridge University Press.

Shensa M. J., The discrete Wavelet Transfrom: Wedding the Á trous and Mallat algorithms, IEEE TRANS. On Siginal Processing, Vol 40(10):2464-2482, 1992.

Starck J.-L., Murtagh F., (1988) Image filtering by combining multiple vision models, http://www.mathsoft.com/signal_processing.htm

Wang, P., (1998). Applying Two Dimensional Kalman Filtering on Digital Elevation Models*, International Archives of Photogrammetry and Remote Sensing,* Vol.32, Part 4, pp649-656.

Wang Zhijun, (2000) Wavelet Transform Based Multi-sensor Remote Sensing Image Fusion, PhD thesis, Wuhan University, P.R.China.